P41 Automated Storm-based Scheduling on the National Weather Radar Testbed Phased Array Radar

David L. Priegnitz
Cooperative Institute for Mesoscale Meteorological Studies, University of Oklahoma, Norman, OK
NOAA/National Severe Storms Laboratory

1. INTRODUCTION

Phased array antennas provide superior scanning ability over conventional mechanical rotating dish antennas. Electronic beam steering allows specific areas in space and time to be scanned without being constrained by the physical position of the antenna. An immediate benefit is to reduce scan update times, providing faster updates of developing and severe weather. Heinselman et al. (2008) used the National Weather Radar Testbed (NWRT) Phased Array Radar (PAR) to demonstrate the benefits of faster scan update times in the detection and monitoring of severe weather. In their study, faster update times were primarily achieved by scanning in a 90º sector rather than a typical 360º sweep. It would be expected that comparable operational phased array radar would use 4 independent antennas to complete a full 360º sweep. Heinselman et al. (2012) further studied the impacts of rapid-scan radar data on the NWS warning decision process and its positive benefits.

One concept that is being explored for future weather and aircraft surveillance is to combine both functions into a single radar (Weber et al., 2007). Scan time, shared between both functions, would reduce the scan update frequency for the weather function, potentially impacting the warning decision process. Since phased array antennas have the ability to electronically steer the beam anywhere within its field of view, the impact of time sharing on the weather detection function could be mitigated by scanning in selected regions. Heinselman and Torres (2011) describe a technique used by the NWRT PAR to identify beams containing precipitation, scanning them more frequently than beams not containing precipitation. The technique is most effective when weather is distant from the radar and isolated, reducing the impact of sharing both weather and aircraft tracking functions in that scenario. However, when weather is close to the radar and/or widespread, this technique provides little or no time savings.

Priegnitz and Heinselman (2013), using the NWT PAR, described a method that identifies storm clusters from reflectivity data. The sectors containing the most intense storm clusters could be targeted for focused scanning, providing faster updates in those sectors. Other sectors, containing less intense, or no precipitation, could be scanned less frequently. On multifunction phased array radars, the cost of sharing time with the aircraft tracking function during severe weather could be reduced through focused storm sector scanning.

Manual identification and selection of candidate storms for focused sector scanning could be a complex and time consuming task. The rest of this paper describes a process, developed for the NWRT PAR, to automatically select candidate storms based on intensity and schedule the sector containing them for focused scanning.

2. FOCUSED SCANNING PROCESS

An adequate description of the focused scanning process used by the NWRT PAR first requires a brief overview of the system architecture. The NWRT PAR system architecture consists of three main components: an environment processor (Henselman and Torres, 2011), a radar control interface (Priegnitz et al., 2007, 2009, 2012), and a real-time controller. The radar control interface (RCI) is a Java-based pair of applications that are used to control and monitor the rest of the system. A server application serves as the focal point for receiving status, products, controlling, and

Corresponding author address: David L Priegnitz, 120 David L. Boren Blvd., Norman, OK 73072.
E-mail: daid.priegnitz@noaa.gov

routing commands to the other components. One or more client applications serve as the bridge between the system and human operators. There can be only a single active, controlling client; while there can be one or more passive, non-controlling clients. The environmental processor consists of a collection of applications running on multiple computer nodes that ingest raw time series data, producing high quality moments used by other system applications. The real-time controller is a single processor that controls the radar hardware. Scanning is initiated by either an active RCI client or by an algorithm running at the server. Time series data are collected by the real-time controller and sent to the environmental processor where it is processed into filtered spectral moments and used by other tasks such as product generation, cluster identification, etc.

Beginning in 2004, a major upgrade was made to the radar control and environmental processor hardware and software providing a platform capable of longer, more robust, data collections that defined the framework used in future upgrades. Since 2007 the NWRT PAR has gone through a regular progression of hardware and software upgrades (Torres et al. 2009, 2010, 2011, 2012, 2013). The most recent software upgrades have focused on the adaptive storm-based scanning process, including: storm cluster identification (Priegnitz and Heinselman, 2013), a range-based VCP algorithm (Priegnitz et al. 2014), implementation of the WSR-88D hail detection algorithm defined by Witt et al. (1998), and an algorithm to automatically schedule a storm

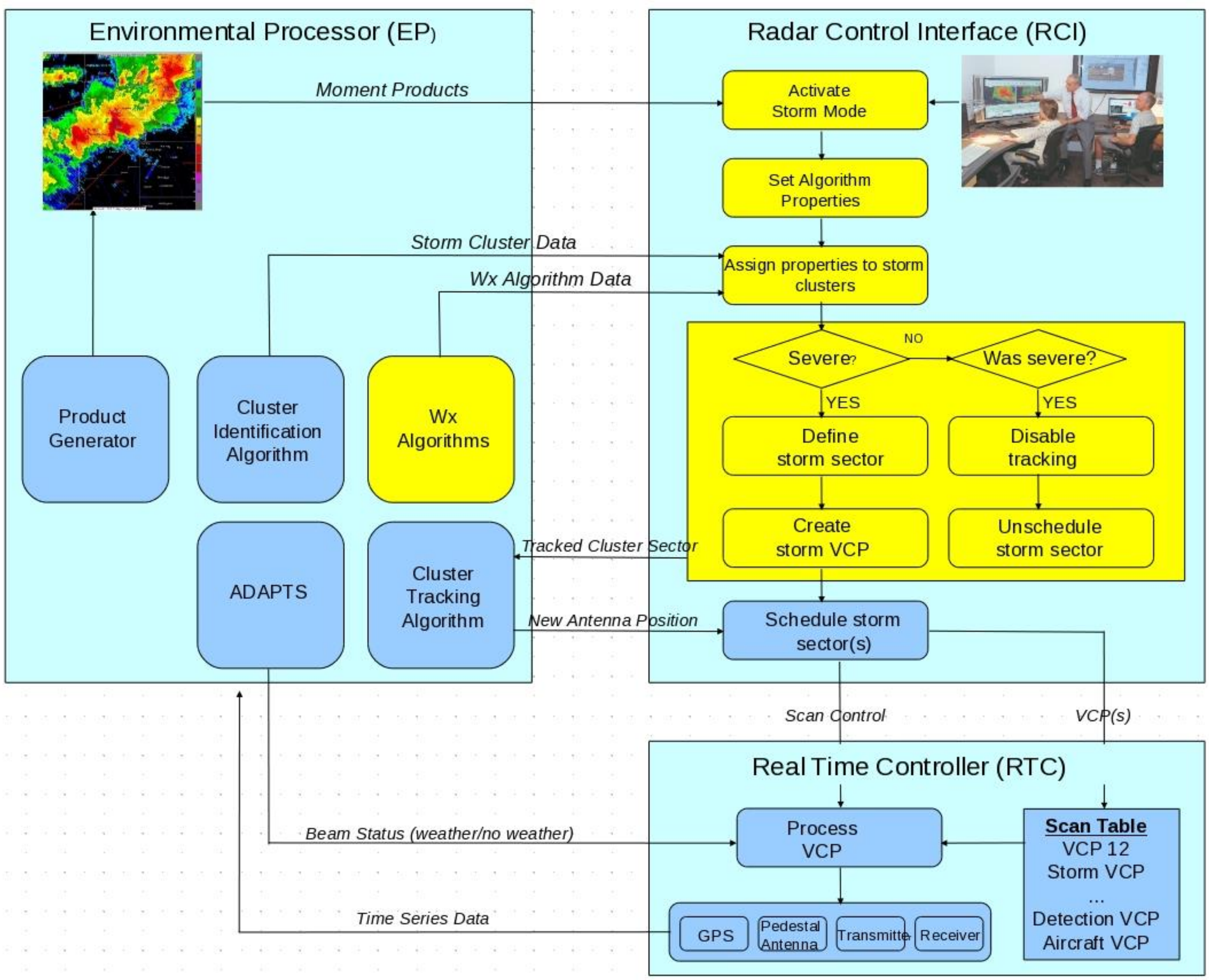

Fig. 1: Functional diagram of the adaptive scanning process at the NWRT PAR. Yellow regions highlight areas involved in the algorithm controlled part of the process.

sector based on storm cluster properties.

A diagram showing the functional NWRT components and their roles in the adaptive scanning process is presented in Fig. 1. The yellow objects represent the major areas involved in the automated storm selection and scheduling process that are the focus of this paper. The focused scanning process can be defined by the following steps: identification, selection, and scheduling

2.1. Storm Identification

Storms are identified by the Cluster Identification Algorithm (Priegnitz and Heinselman, 2013) using a watershed technique, described by Lakshmanan et al (2009) to group adjacent reflectivity gates containing precipitation into objects, or storm clusters. The use of two reflectivity thresholds eliminates weak echoes and identifies stronger storm clusters. A choice of constant elevation (PPI) or constant height (CAPPI) reflectivity data are used as input. PPI data have an advantage in that an entire volume coverage pattern (VCP) doesn't have to be completed before performing the cluster analysis; only one complete elevation scan. This allows the storm selection and scheduling functions to be completed prior to the start of the next VCP. A disadvantage is that discrete storm cells may be difficult to distinguish at low elevation angles in a complex environment (i.e. squall line). CAPPI data have a disadvantage in that a completed VCP is required before starting the cluster analysis; the cluster analysis won't be completed until well into the execution of the next VCP cycle. However, analysis of several archived NWRT data sets suggest that the identification of discrete storm cells in a complex environment can be improved using a constant height rather than a slant angle. Both input types work equally well in isolated convective environments.

2.2. Storm Selection

Storm selection begins by searching reflectivity, velocity, and derived products for severe or developing severe, weather. The process can be time consuming for a human operator, negatively impacting the warning decision process; especially in an environment with multiple candidate storm clusters.

To address this issue, a set of algorithm generated properties have been developed for the NWRT PAR that can be used to identify severe, or potentially severe, storm clusters. A recent enhancement to the cluster identification algorithm constructs a composite vertical reflectivity profile, in half kilometer intervals from the surface to 20 km, for each storm cluster. These profiles, in conjunction with the 0º C and -20º C height levels, are used by the recently added hail detection algorithm to determine the maximum expected hail size (MEHS) for each storm cluster. A database of cluster properties is maintained at the RCI server and used in the storm selection process (it is expected that additional profiles and properties will be added in the future).

2.3. Storm Sector Scheduling

Once a storm cluster has been identified and selected for focused scanning (either by an algorithm or human operator), an algorithm at the RCI server creates a range-based VCP (Priegnitz et al., 2014) that is sent to the real-time controller and added to the scan table. The scan table contains up to 10 distinct weather VCPs which are executed in a round-robin fashion (Priegnitz and Heinselman 2013). A new “storm mode” has been incorporated into the real-time controller software, allocating an operator defined segment of time exclusively for storm VCPs (Priegnitz et al. 2015). Storm VCPs are executed in a round-robin fashion within this time segment. When storm mode is activated, the scan table will contain one weather surveillance and one or more storm VCPs. When scanning is initiated, the weather surveillance VCP is executed first. Upon completion, a timer is started prior to executing the first storm VCP. When the last storm VCP in the list is completed the timer is checked. If the elapsed time is less than the time segment the storm VCP list is repeated. If not, a new weather surveillance VCP is started and the entire process repeated. Storm mode is terminated when there are no longer any active storm VCPs in the scan table or if scanning is terminated by the operator. For example, a scan sequence containing two storm VCPs is presented in Table 1. A time segment of 120 seconds is defined for focused storm scanning. Following the execution of the weather surveillance VCP (Enhanced VCP 12), storm VCPs 1 and 2 are repeated until after the eighth storm VCP cycle (the elapsed storm time is 126 seconds). At that time scanning returns to the weather surveillance VCP and the process repeated.

VCP	Volume Time (s)	Storm Timer (s)	Elapsed Time (s)
Enhanced VCP 12	38	0	0
Storm 1	6	0	38
Storm 2	9	6	44
Storm 1	6	15	53
Storm 2	9	21	59
Storm 1	6	30	68
Storm 2	9	36	74
Storm 1	6	45	83
Storm 2	9	51	89
Storm 1	6	60	98
Storm 2	9	66	104
Storm 1	6	83	113
Storm 2	9	89	119
Storm 1	6	96	128
Storm 2	9	102	134
Storm 1	6	111	143
Storm 2	9	117	149
Enhanced VCP 12	38	126	158
Storm 1	6	0	196
Storm 2	9	6	202

Table 1: Sample storm mode scan sequence with two active storm sectors. The storm timer is set to 2 minutes. The timer and elapsed times are at the start of each scan volume.

3. ALGORITHM-CONTROLLED STORM SELECTION AND SCHEDULING

As previously mentioned, the storm selection and scheduling process can be time consuming, negatively impacting the warning decision process if performed entirely by a human operator. Using algorithms to identify, select, and schedule storms could remove much of this burden. As a demonstration, MEHS was selected to be used at the NWRT PAR in the selection and scheduling process.

The RCI server maintains a list of storm clusters that meet an operator defined lower MEHS threshold. After completion of a weather surveillance VCP, new storm cluster profiles are sent to the RCI server and used by the hail detection algorithm to determine the MEHS for each storm cluster. If the MEHS for a storm cluster reaches this lower threshold, it is added to the storm list. If it falls below this threshold it is removed from the list. A upper MEHS threshold is used to identify storm clusters that are candidates for focused storm sector scanning. When this threshold is reached or exceeded, the range of the storm cluster gate with the highest reflectivity is used by the range-based VCP algorithm to create a storm sector VCP. This storm sector VCP is sent to the real-time controller and added to the scan table. Once a storm cluster sector is targeted for focused scanning, it will remain active until either terminated by the operator or when the storm cluster MEHS falls below the average of the two thresholds.

As an example, NWRT PAR data from May 19, 2013 were replayed using lower and upper MEHS thresholds of 2.54 cm (1 inch) and 5.08 cm (2 inch), respectively. On that day, several violent tornadoes occurred in central Oklahoma. Data for the 0ºC (4328 m) and -20ºC (6929 m) levels required by the hail algorithm were extracted from the 1200 UTC Norman (KOUN) sounding. By 153507 CDT (203507 UTC), four storm clusters meeting the 2.54 cm threshold were identified and added to the storm list. Fig. 2 is a snapshot of a RCI client algorithm window at 153507 CDT containing the storm list (left) and 0.5º elevation reflectivity product (right). The storm list contains selected properties for each of the storm clusters, including the MEHS in the rightmost column. Since the MEHS for storm cluster 3 exceeds the 2 inch upper threshold, the sector surrounding it is targeted for focused scanning (check box in “Sched” column set). The scan table at this time contains 2 VCPs, one weather surveillance and one storm VCP. A profile of the algorithm generated VCP for the sector containing storm 3 is shown in Fig. 3. This VCP contains 22 elevation angles, with red lines indicating split cut (two PRT) and

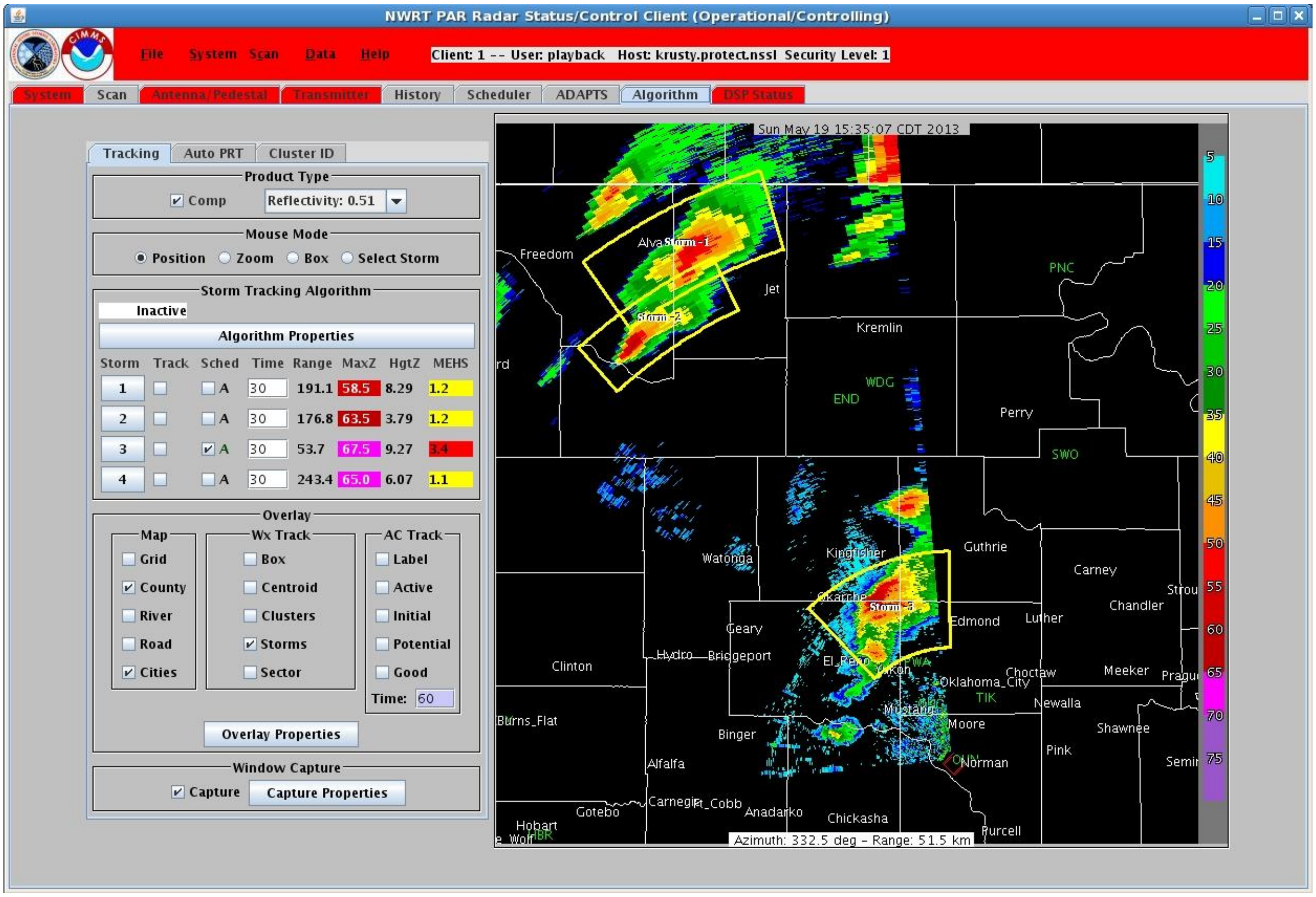

Fig. 2: RCI Client Algorithm tab panel display. Algorithm and display control objects are displayed on the left and moments displayed on the right. Moments can be displayed by elevation (PPI) or height (CAPPI). The Storm Tracking Algorithm group contains a list of storms meeting an operator defined MEHS threshold (2.54 cm).

green lines uniform (single PRT) waveform elevations.

To provide an operator with a more holistic view of storm clusters and their evolution, a new "storm cluster profile" display was added to the RCI client. This display includes a scan by scan vertical profile of composite reflectivity, maximum reflectivity, maximum reflectivity height, along with a plot of MEHS. An operator can select any storm in the reflectivity display (Fig 2). If a storm cluster can be matched to the selected location a storm cluster profile is generated and displayed as a pop up window. The profile is updated whenever a new cluster profile is received by the RCI server.

An example storm cluster profile for storm 3 at 153507 CDT is presented in Fig. 4. The history for storm 3 begins at 143718 CDT and continues to the most recent scan at 153507 CDT. The storm cluster did not meet minimum reflectivity or size thresholds for a period of time between 143718 CDT and 144554 CDT, accounting for the gap in the storm cluster profile. The vertical scan-by-scan reflectivity profile is displayed in the upper portion of the window. The vertical reflectivity profile clearly shows how this storm went through several growth/decay cycles before becoming severe (maximum reflectivity for each scan is displayed as a label at the height of occurrence). The two solid red horizontal lines represent the heights of the 0º C (lower) and -20º C (upper) levels from the sounding. Maximum echo height continued to increase steadily throughout the period as well as the maximum reflectivity. The MEHS profile is displayed at the bottom of the cluster profile window. During the second growth cycle after 145554 CDT the MEHS reached the lower threshold (yellow) for 2 volume scans before dropping below it (gray). At those times the storm would have been visible in the storm list. Finally, around 151000 CDT the storm once

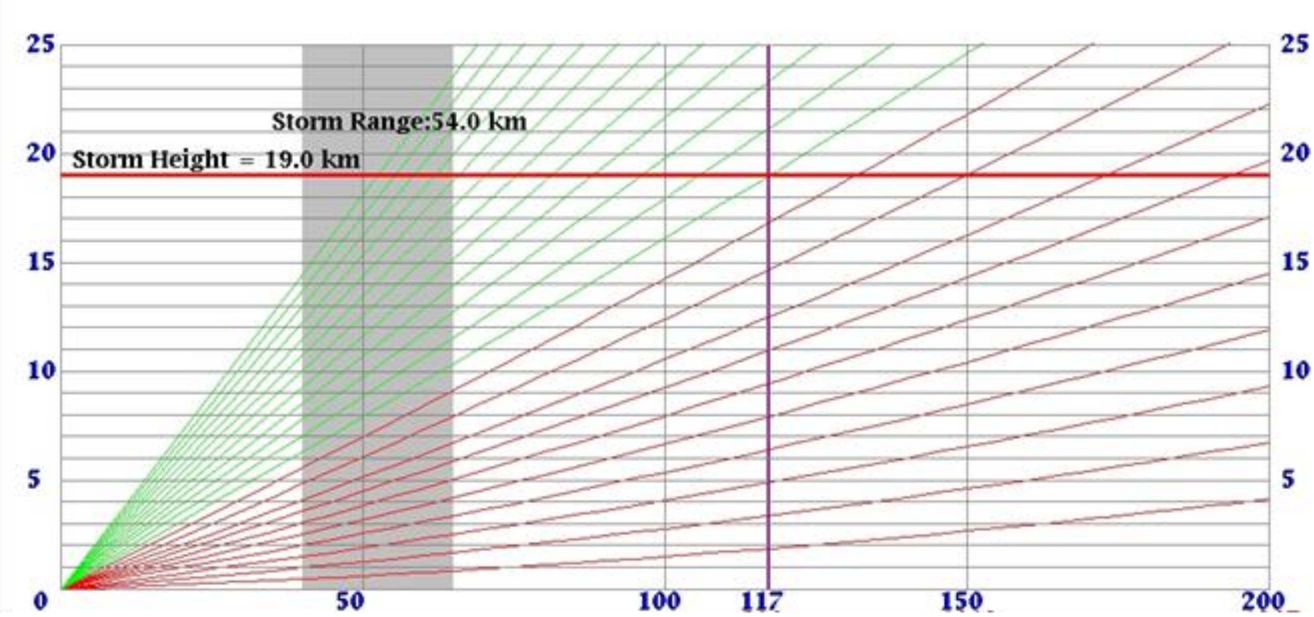

Fig. 3: Volume coverage pattern (VCP) generated by the range-based VCP algorithm for storm 3 at 153507 CDT. Red lines represent split cut (two PRTs) and green uniform (single PRT) waveforms.

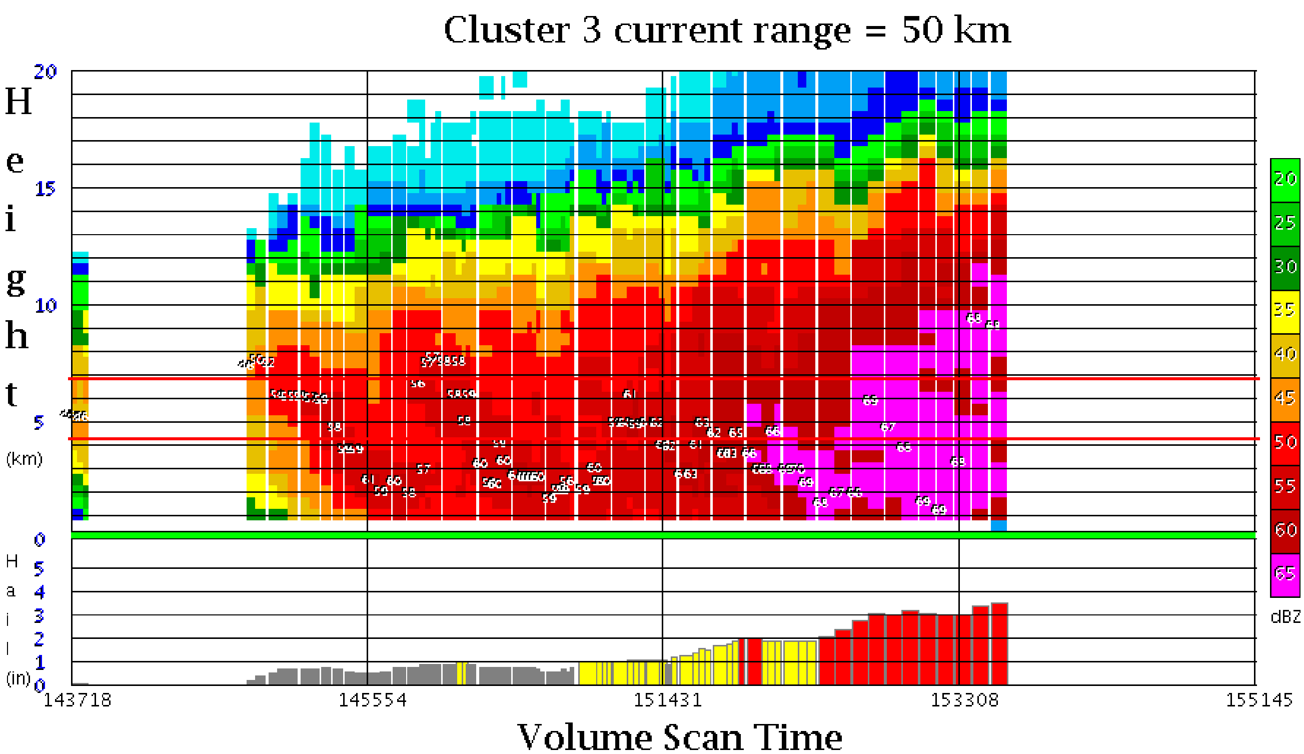

Fig. 4: Storm cluster profile display window for storm 3 at 153507 CDT. The top graph shows the maximum storm cluster reflectivity from the lowest elevation to storm top in half kilometer increments. The width of a vertical column corresponds to the volume scan time. The label in each column indicates the maximum reflectivity and is plotted at the height of occurrence. The bottom graph shows the scan by scan maximum expected hail size (MEHS). It is color coded as follows: gray < 1 in; yellow >= 1 in and < 2 in; red >= 2 in.

again reached the lower MEHS threshold (yellow) and would have been in the storm list thereafter. As the storm increased in size and intensity the sector containing it would have been targeted for focused scanning at the time the MEHS reached 5.08 cm (red), remaining targeted through the latest volume scan.

4. SUMMARY

With the possibility of future multifunction radars performing both aircraft and weather surveillance functions it is important to develop new weather scanning techniques that minimize the impact of sharing time with the aircraft function. Several adaptive scanning techniques have been developed for the NWRT PAR to focus scanning on regions containing precipitation. The technique presented in this paper focuses on the most dynamic precipitation regions. Due to the complex nature of storm identification, selection, and scheduling, an automated algorithm controlled method was demonstrated which could be used as the framework for future weather scanning on multifunction radars. In this paper, MEHS thresholds were used for storm selection and scheduling. One would expect that the storm selection and scheduling process would consider many additional storm properties not included in this study.

5. ACKNOWLEDGEMENT

Support for this paper and research was provided by NOAA/Office of Atmospheric Research under NOAA-University of Oklahoma Cooperative Agreement #NA11OAR4320072, U.S. Department of Commerce. The statements, findings, conclusions, and recommendations are those of the author and do not necessarily reflect the views of NOAA and the U.S. Department of Commerce.

REFERENCES

Heinselman, P. L., D. L. Priegnitz, K. L. Manross, T. M. Smith, and R. W. Adams, 2008: Rapid sampling of severe storms by the National Weather Testbed Phased Array Radar. Wea. Forecasting, **23**, 808-834.

Heinselman, P. L., and S. M. Torres, 2011: High-temporal resolution capabilities of the National Weather Radar Testbed phased array radar. J. Appl. Meteor. Climatol., 50, 579-593.

Heinselman, L. L., D. S. LaDue, and H. Lazrus, 2012: Exploring impacts of rapid-scan radar data on NWS warning decisions, Wea. Forecasting, **27**, 1031-1044.

Lakshmanan, V., K. Hondl, and R. Rabin, 2009: An efficient, general-purpose technique to identify storm cells in geospatial images. J. of Atmos. And Oceanic Tech., **26**, 523-537.

Priegnitz, D. L., P. L. Heinselman, and C. D. Curtis, 2007: Dynamic scanning for the National Weather Radar Testbed, Extended Abstract, 33rd Conf. on Radar Meteor., Cairns, Australia, Amer. Meteor. Soc., P7.3.

Priegnitz, D. L., P. L. Heinselman, S. M. Torres, and R. Adams, 2009: Improvements to the National Weather Radar Testbed Radar Control Interface, Extended Abstract, 34th Conf. on Radar Meteor., Williamsburg, VA, Amer. Meteor. Soc., P10.10.

Priegnitz, D. L., S. M. Torres, and P. L. Heinselman, 2012: An adaptive pedestal control algorithm for the National Weather Radar Testbed phased array radar. Extended Abstract, 28th Conf. on Interactive Information and Processing Systems (IIPS) for Meteorology, Oceanography, and Hydrology, New Orleans, LA, Amer. Meteor. Soc., P8.2.

Priegnitz, D. L., S. M. Torres, and P. L. Heinselman, 2013: Enhancements to the National Weather Radar Testbed phased array radar storm tracking function. Extended Abstract, 29th Conf. on Environ. Info. Proc. Tech., Austin, TX, Amer. Meteor. Soc., P19.

Priegnitz, D. L. and P. L. Heinselman, 2013: Detection and adaptive scheduling on the NWRT phased-array radar. Extended Abstract, 36th Conf. on Radar Meteor., Breckinridge, CO, Amer. Meteor. Soc., P147.

Priegnitz, D., P. Heinselman, and R. Brown, 2014: Adaptive storm-based scanning at the National Weather Radar Testbed phased array radar. Extended Abstract, 8th European Conf. on Radar in Meteor. And Hydro., Garmisch-Pertenkirchen, Germany, TEC.P09.

Priegnitz, D. L., P. L. Heinselman, and R. A. Brown, 2015: Adaptive multiple storm-based scanning at the National Weather Radar Testbed phased array radar. Extended Abstract, 37th Conf. on Radar Meteor., Norman, OK, Amer. Meteor. Soc., P11.

Torres, S., C. Curtis, I. Ivic, D. Warde, E. Forren, J. Thompson, D. Priegnitz, and R. Adams, 2009: Update on the signal processing upgrades for the National Weather Radar Testbed. Extended Abstract, 25th Int. Conf. on Interactive Information and Processing Systems (IIPS) for Meteorology, Oceanography, and Hydrology, Phoenix, AZ, Amer. Meteor. Soc., P8B.4.

Torres, S., C. Curtis, I. Ivic, D. Warde, E. Forren, J. Thompson, D. Priegnitz, and R. Adams, 2010: Update on the signal processing upgrades for the National Weather Radar Testbed. Extended Abstract, 26th Int. Conf. on Interactive Information and Processing Systems (IIPS) for Meteorology, Oceanography, and Hydrology, Atlanta, GA, Amer. Meteor. Soc., P14B.2.

Torres, S., C. Curtis, I. Ivic, D. Warde, E. Forren, J. Thompson, D. Priegnitz, and R. Adams, 2011: Update on the signal processing upgrades for the National Weather Radar Testbed. Extended Abstract, 27th Int. Conf. on Interactive Information and Processing Systems (IIPS) for Meteorology, Oceanography, and Hydrology, Seattle, WA, Amer. Meteor. Soc., P12B.3.

Torres, S., P. Heinselman, R. Adams, C. Curtis, E. Forren, I. Ivic, D. Priegnitz, J. Thompson, and D. Warde, 2012: Software and signal processing upgrades for the National Weather Radar Testbed phased-array radar. Extended Abstract, 28th Int. Conf. on Interactive Information and Processing Systems (IIPS) for Meteorology, Oceanography, and Hydrology, New Orleans, LA, Amer. Meteor. Soc., P6B.3.

Torres, S., R. Adams, C. Curtis, E. Forren, I. Ivic, D. Priegnitz, J. Thompson, and D. Warde, 2013: New weather-surveillance capabilities for NSSL's phased-array radar. Extended Abstract, 29th Conf. on Environmental Information Processing Technologies, Austin, TX, Amer. Meteor. Soc., P8.3.

Weber, M., J. Cho, J. Herd, J. Flavin, W. Benner, and G. Totok, 2007: The next-generation multimission U.S. Surveillance radar network. Bull. Amer. Meteor. Soc., **88**, 1739-1751.

Witt, A., M. D. Eilts, G. J. Stumpf, J. T. Johnson, E. D. Mitchell, and K. W. Thomas, 1998: An enhanced hail detection algorithm for the WSR-88D. Weather and Forecasting, **13**, 286-303.